

High-field current transport and charge trapping in buried oxide of SOI materials under high-field electron injection

Alexei N. Nazarov, Yuri Houk, and Valeriya I. Kilchytska

Abstract — Mechanisms of the charge transfer, the charge trapping, and the generation of positive charge during the high-field electron injection into buried oxide of silicon-on-insulator structures fabricated by different technologies are analyzed based on the data obtained from current-voltage, injection current-time, and capacitance-voltage characteristics together with SIMS data. Electron injection both from the Si film and the Si substrate is considered. The possibility of using the trap-assisted electron tunneling mechanisms to explain the high-field charge transfer through the buried oxides of UNIBOND and SIMOX SOI materials is considered. It is shown that considerable positive charge is accumulated near the buried oxide/substrate interface independently from the direction of the injection (from the film or from the silicon substrate) for UNIBOND and SIMOX SOI structures. Thermal stability of the charge trapped in the buried oxides is studied at temperatures ranging from 20 to 400°C. The theory is compared with the experimental data to find out the mechanisms of the generation of positive charge in UNIBOND and SIMOX buried oxides.

Keywords — Fowler-Nordheim current, trap-assisted tunneling, silicon-on-insulator, buried oxide, SIMOX, UNIBOND, anode hole injection, band-to-band impact ionization.

1. Introduction

Silicon-on-insulator (SOI) structures are intensively introduced in large-scale fabrication of reliable integrated circuits and devices. The reliability and stability of such devices strongly depend upon the quality of the buried oxide (BOX) layer and its interfaces. This is especially important for such an attractive application of SOI as high-power devices, where the processes of charge injection into the BOX play a key role in the stability of operation. It is known [1] that the electrical and structural properties of the buried oxide silicon interfaces in SIMOX SOI structures are worse when compared to those of the gate oxide/silicon ones. This, in turn, results in increased charge trapping in the BOX and its degradation during SOI device operation, especially at high voltages. Such behavior often limits promising prospective applications of SOI structures, especially for high-voltage and high-temperature devices. Thus in the present work we study the nature of electrical conductance, charge trapping and positive charge generation processes in the BOX of SOI substrates made using the two most advanced technologies, namely UNIBOND® and SIMOX. Possible mechanisms of charge injection and

positive charge build-up into the BOX of the SIMOX and experimental UNIBOND SOI wafers during high-field electron injection are discussed.

2. Experimental

The experimental UNIBOND SOI structures were fabricated by CEA-LETI using the Smart Cut® process [2]. UNIBOND structures were made on p-type silicon substrates with the doping level of $6.5 \cdot 10^{13} \text{ cm}^{-3}$. The thickness of buried oxide and silicon film was 400 and 200 nm, respectively.

The SIMOX SOI structures were formed on p-type Si with the doping of $8 \cdot 10^{14} \text{ cm}^{-3}$ by means of a single implantation process with the oxygen dose of $1.8 \cdot 10^{18} \text{ O}^+/\text{cm}^2$, beam energy of 200 keV at 600°C. In the following these SOI structures will be denoted simply as SIMOX ones. Post implantation annealing was performed at 1320°C in an Ar+2%O₂ ambient for 6 hours. The thickness of the BOX and the silicon film was 360 and 200 nm, respectively.

For the purposes of electrical investigation SOI capacitors were formed by mesa isolation. The investigated Al-Si-SiO₂-Si mesa capacitors had variable areas, ranging from 0.95 to $2.75 \cdot 10^{-3} \text{ cm}^2$.

Electrical injection into the BOX was performed using constant voltage stress at electric fields in the range of 3–7 MV/cm. Both positive and negative stress voltages were applied to the silicon film, so that electrons were injected from the silicon substrate and the silicon film, respectively. During such injection current vs. time (*I-t*) measurements were performed. Other electrical characterization has been carried out by means of high-field current-voltage (*I-V*) and high-frequency (1 MHz) capacitance-voltage (*C-V*) techniques.

3. Results and discussion

3.1. High-field electron injection

As seen in Fig. 1a, both experimental UNIBOND and SIMOX SOI structures exhibit asymmetry in high-field conduction, which indicates different quality of the BOX/film and the BOX/substrate interfaces. Indeed, in a lot of studies devoted to the investigation of the material quality and defects in SIMOX structures it was shown that the BOX

contains a great number of silicon inclusions [3], crystalline coesite phase of SiO_2 [4, 5], as well as dangling [6] and strained [7] bonds, all located predominantly near the BOX/substrate interface. The presence of these defects may result in worse electrical properties of this interface compared to those of the BOX/film interface. In the case of the experimental UNIBOND structure the bonding of the initial wafers occurs at the bottom BOX interface [2] (i.e. at the BOX/substrate interface). It is thus natural to suggest that its electrical properties are somewhat worse than those of the top BOX interface. In fact, as seen in Fig. 1a, the threshold voltage of high-field electron injection from the substrate is much lower than that from the film for both experimental UNIBOND and SIMOX structures, attesting to the inferior electrical quality of the BOX/substrate interface in both structures.

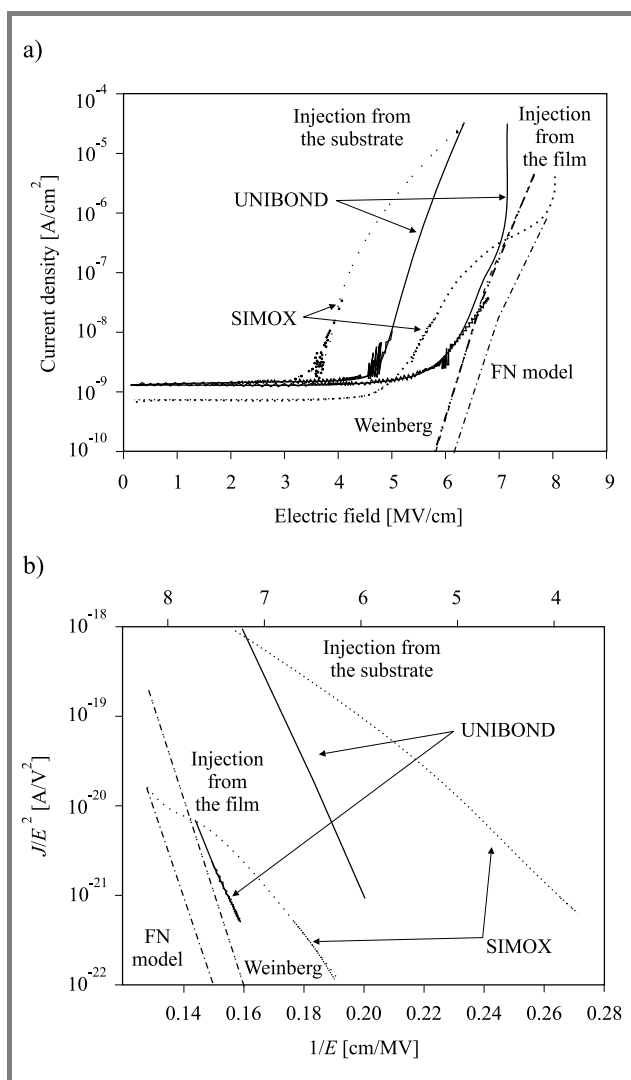


Fig. 1. Current-voltage characteristics of the experimental UNIBOND and SIMOX SOI structures: (a) standard coordinates; (b) Fowler-Nordheim plot. Theoretical curves describing the tunneling current in the BOX of the experimental UNIBOND structure calculated according to the Fowler-Nordheim [9] and Weinberg [10] models are also presented.

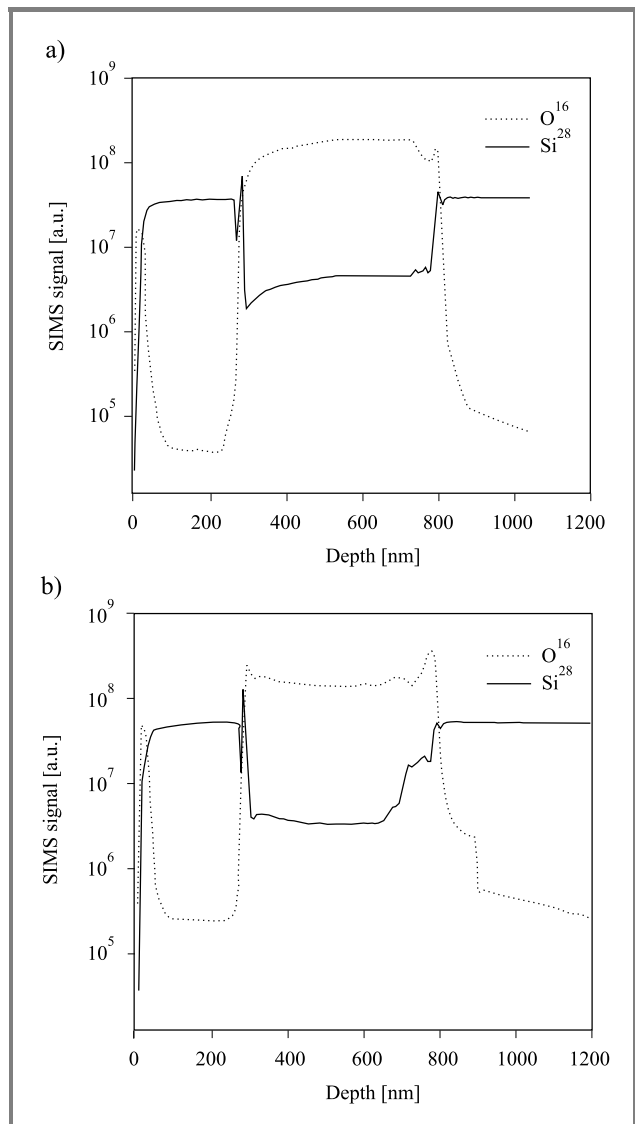


Fig. 2. SIMS investigations of UNIBOND (a) and SIMOX (b) SOI structures.

Indeed, SIMS measurements of atom distribution in the BOX, presented in Fig. 2, indicate the presence of non-stoichiometric composition near the BOX/silicon substrate interface for both experimental UNIBOND and SIMOX structures. It should be noted that in the case of SIMOX structures, considerable increase of Si atom concentration is observed at a distance of more than 100 nm from the BOX/silicon substrate interface (Fig. 2b). Such increase of Si concentration can be associated with silicon inclusions, observed in BOX of similar SIMOX material [3] near the BOX/substrate interface. The nature of such inclusions in the BOX has been proposed in the paper by Afanas'ev *et al.* [8]. In the case of experimental UNIBOND SOI structures, detectable decrease of oxygen atom concentration in the BOX at the distance of 50 nm from the BOX/substrate interface has been found. Since this interface is the bonded one we can suggest that the decrease of

oxygen concentration in this region could be associated with oxygen outdiffusion into the bonded interface. Additionally, it should be noted that the observed non-stoichiometry of the BOX near the BOX/Si substrate interface in the case of UNIBOND material is considerably lower than that of the SIMOX material.

The high-field electric conduction curves of both UNIBOND and SIMOX structures are almost linear in the Fowler-Nordheim (FN) coordinates (Fig. 1b). This attests that the dominant conduction mechanism in both cases is electron tunneling from cathode to the BOX through a triangular potential barrier. This assumption is also supported by a weak temperature dependence of high-field conductivity.

By the classical FN theory the current density, J_{FN} , can be written as [9]:

$$J_{FN} = C \cdot E_c^2 \cdot \exp\left(-\frac{\beta \cdot \Phi^{3/2}}{E_c}\right), \quad (1)$$

where $C = \frac{e^3 m_0}{8\pi h m^* \Phi}$ and $\beta = \frac{4\sqrt{2m^*}}{3e\hbar}$. E_c is the electric field in the BOX near the cathode, Φ is the potential barrier height, m_0 is the mass of free electron in vacuum, m^* is the effective electron mass in SiO₂ band gap ($m^* = 0.5m_0$), other values have their usual meaning.

Thus the application of the simple FN analysis to the I-V characteristics allows the determination of the effective potential barrier heights for electron emission from the silicon film and the silicon substrate into the BOX. The obtained values of the effective barrier heights (Φ_{FN}) and the threshold electric field of high-field electron injection (E_{th}) for both interfaces of the experimental UNIBOND and SIMOX materials are summarized in Table 1.

Table 1

Effective barrier heights (Φ_{FN}), calculated by using FN analysis, and threshold electric fields (E_{th}) of high-field electron injection into the BOX from the silicon film and the substrate in different SOI structures

Material	Direction of injection	Φ_{FN} [eV]	E_{th} [MV/cm]
UNIBOND	Film	2.4	5.8
	Substrate	2.3	4.8
SIMOX	Film	1.3	4.7
	Substrate	1.2	3.3
Gate oxides	Si substrate [9]	2.9	6.0
	Si substrate [11]	3.1	6.0

In both cases (SIMOX and experimental UNIBOND structures) the effective barrier heights for the BOX/film interface (about 1.3 and 2.4 eV, respectively) are higher than those for the BOX/Si substrate interface (about 1.2 and 2.3 eV, respectively) indicating worse electrical properties of the BOX/substrate interface for both materials. However, for the experimental UNIBOND SOI structures the effective potential barrier heights are considerably higher

than those observed in SIMOX, and slightly below the typical values obtained for gate oxides (2.9–3.1 eV) [11, 12]. Moreover, the threshold electric field of high-field electron injection from the Si film into the BOX of the experimental UNIBOND material is just the same as for good thermal oxide (see Table 1). Thus, the electrical properties of the Si film/BOX interface in the experimental UNIBOND structure are just similar to those of the gate oxide/silicon interface.

Reduced values of the potential barrier heights determined by the FN analysis of the I-V characteristics of both the experimental UNIBOND and SIMOX structures indicate that the mechanism of charge transfer through the BOX differs in some way from the ordinary FN mechanism. The observed decrease of the effective potential barrier heights for high-field electron injection from Si into the BOX for the studied SOI structures should be interpreted as an increase of the probability of electrons tunneling from Si into the BOX as compared with that of electrons tunneling from Si into gate oxide for metal-thermal oxide-silicon (MOS) structures. In order to explain such effects in [13] a model, considering the appearance of interfacial asperities, has been developed. However, for the experimental UNIBOND structures this approach is physically unjustified, especially for the Si film/BOX interface, and for the SIMOX structures the use of this approach gives unreasonable large values of asperity separation [14].

We suggest that an increase of the probability of electron tunneling through the potential barrier in the case of the SOI BOX can be connected to the trap-assisted tunneling (TAT) mechanism [15].

TAT model employment. In the case of the TAT mechanism the slope of the high-field I-V characteristic (and therefore the threshold electric field), presented in FN coordinates, is linked to the energetic position of a trap in the oxide band gap ϕ_t , while its intercept is connected both with the energetic position and the trap concentration N_t . Therefore, we can numerically fit TAT current to our experimental data, which allows us to extract trap parameters.

Direct employment of the TAT model yields unreliable values of trap concentrations in the experimental UNIBOND, as well as SIMOX, structures for injection at both interfaces.

Due to a high quality of the silicon film/BOX interface it is necessary in the case of the experimental UNIBOND material to take into account the possibility of direct FN tunneling of electrons from the silicon film into the BOX simultaneously with the trap-assisted tunneling. Indeed, Fig. 1a demonstrates that the experimental I-V characteristics of the electron injection from the silicon film into the BOX of the experimental UNIBOND structure are close enough to the classical FN curve calculated according to (1). Equation (1) was, however, initially derived [9] for the case of electrons tunneling from a metal into vacuum, and is based on the Sommerfeld model of metal. In this model the free electrons are assumed to form a three-

dimensional Fermi gas. In our case of tunneling from semiconductor into the BOX at high fields, however, very strong band banding at the Si-SiO₂ interface is observed, therefore we have a large density of electrons which are confined to a narrow layer at this interface. Such layers have been studied extensively and have been characterized by a two-dimensional model with quantized levels or subbands [16]. Weinberg showed [10] that the tunneling current from the lowest discrete subband may be expressed as follows:

$$J_B(E_0) = \theta \left[1.13 \left(1 + \frac{m_{ox}}{m_s} \frac{E_0}{e\phi_B} \right)^{-1} \right] \sqrt{\frac{e m_{ox}}{m_s \phi_B} \frac{\epsilon_{ox}^2}{\epsilon_s} F^2} \times \exp \left[-\frac{\beta(\phi_B - E_0)}{F} \right] = C_W F^2 \exp \left[-\frac{\beta(\phi_B - E_0)}{F} \right], \quad (2)$$

where $\theta = 0.626$ is the fraction of carriers in this subband, $E_0 = 0.209$ eV is the energy of this subband relatively to the edge of semiconductor conduction band at the interfaces.

One can see from Fig. 1a that this current is much closer to the experimental current of electrons injected from Si film into the BOX of UNIBOND structure than the classical FN one and its subtraction from the experimental data yields a significantly different curve. If the TAT model is fit to the result of this subtraction, one obtains a reasonable estimation of trap parameters in the BOX of the experimental UNIBOND structures in the vicinity of the Si film/BOX interface: $\phi_t = 1.48$ eV, $N_t = 4.38 \cdot 10^{15} \text{ cm}^{-3}$.

For the injection from the Si substrate into the BOX of the experimental UNIBOND material we obtain good approximation $\phi_t = 0.82$ eV, $N_t = 2.78 \cdot 10^{18} \text{ cm}^{-3}$ by assuming a 0.5 eV lowering of the potential barrier at the Si substrate/BOX interface due to worse quality of this interface (see the discussion of the SIMS results). Thus we obtained a lower trap concentration in the vicinity of the BOX/silicon film interface than in the vicinity of the BOX/substrate interface, which is physically justified.

As seen in Fig. 1b, the high-field I-V characteristics of SIMOX structures differ significantly from straight lines when plotted in FN coordinates. It should be noted, however, that it is possible to split them into two straight-line sections (Fig. 3). Thus, we suppose that there are two stages in the process of electron injection into the BOX of SIMOX structure, each with different potential barriers. Indeed, classical FN estimations of the effective barrier heights for these sections (Table 2) show that they decrease with the injection time. This indicates that the barriers are dynamically changing during the injection process. Therefore, we suggest the following model. As it is showed below, a significant positive charge is rapidly created in the BOX of a SIMOX structure exposed to high-voltage stress. Moreover, its centroid moves during the injection towards the Si substrate/BOX interface. This charge affects the electric field in the BOX, and the total field differs considerably from the external one. To employ the TAT model properly we have to use just this total field in the BOX in tunneling region.

As the centroid moves toward the substrate/BOX interface during the injection, the shape of the barrier changes [17].

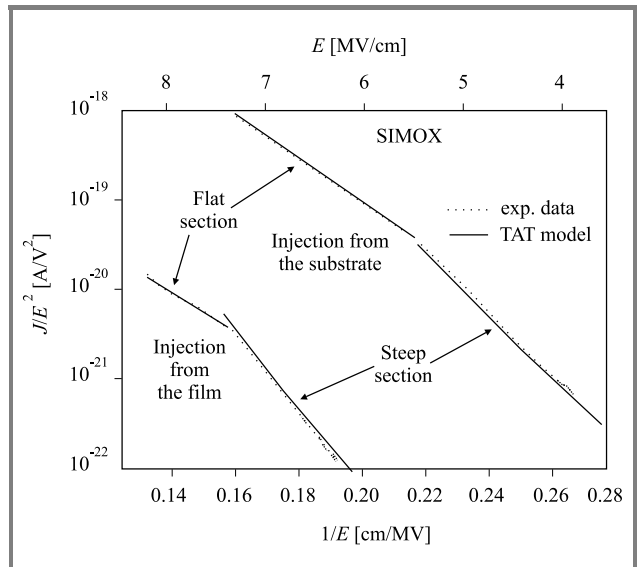


Fig. 3. TAT modeling of high-field injection current into the BOX of SIMOX SOI structure in FN axes.

As a consequence, the tunneling probability changes too, which may cause a distortion of I-V characteristics of SIMOX structures. To estimate trap parameters we fit the first straight (steep) section of the I-V characteristics plotted in FN coordinates, while taking into account the presence of positive charge in the BOX with a fixed centroid. The obtained results are presented in Table 2. The values of

Table 2

Effective barrier heights (Φ_{FN}) for two different sections of high-field I-V characteristics of SIMOX structures and the parameters of traps in the BOX near both interfaces

Interface	Section (see Fig. 3)	Φ_{FN} [eV]	ϕ_t [eV]	N_t [cm^{-3}]
Substrate	Steep	1.4	1.9	$1.6 \cdot 10^{16}$
	Flat	1.1		
Film	Steep	1.6	1.9	$1.4 \cdot 10^{14}$
	Flat	1.0		

trap concentrations are close enough to those of the experimental UNIBOND structure, which does not correlate with other information about the quality of SIMOX BOX. This shows that it is necessary to carry out a more comprehensive analysis of charge injection into such a complicated structure.

3.2. Charge build-up

It is well established that high-field electron injection into thermal oxide [18], BOX of SIMOX [13] and wafer bonding (WB) SOI structures [19] results in electron and hole trapping in these oxides.

High-frequency (HF) C-V measurements along with I-t measurements were used to study the charge trapping

in the buried oxides under high-field electron injection. The C-V technique is more useful in the case of SOI capacitors in comparison with MOS ones, because it allows to obtain more comprehensive information about the charge in the BOX and its changing during the injection due to the possibility of electrical potential control at both interfaces of BOX. Therefore, it is easy to determine the net accumulated charge in the BOX and its centroid [20].

Figures 4a and 5a present the C-V characteristics obtained from the experimental UNIBOND and SIMOX SOI structures before and after electron injection into the BOX from the Si film with injection times up to $2 \cdot 10^4$ s. Similar C-V characteristics are also observed in the case of injection from the Si substrate.

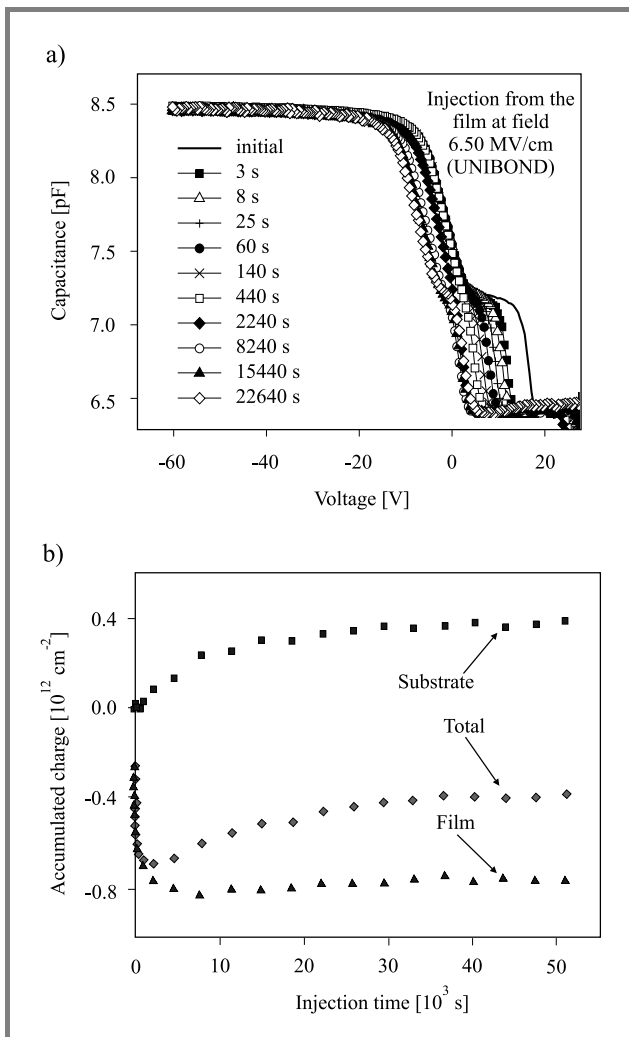


Fig. 4. (a) Capacitance-voltage characteristics of the UNIBOND SOI structure with the electron injection time as a parameter; (b) charge accumulated in the BOX as a function of electron injection time.

The difference in the shape of the C-V plots obtained from the investigated experimental UNIBOND and SIMOX SOI capacitors arises from the difference dopant types of the Si film: n-type in the case of UNIBOND structures and

p-type in the case of SIMOX ones. In spite of the different shape, in both cases the C-V plots exhibit two well-defined regions with varying capacitance related to the changing of the electrical potential at the BOX/substrate interface (negative voltages – left part of the plots) and at the BOX/film interface (positive voltages).

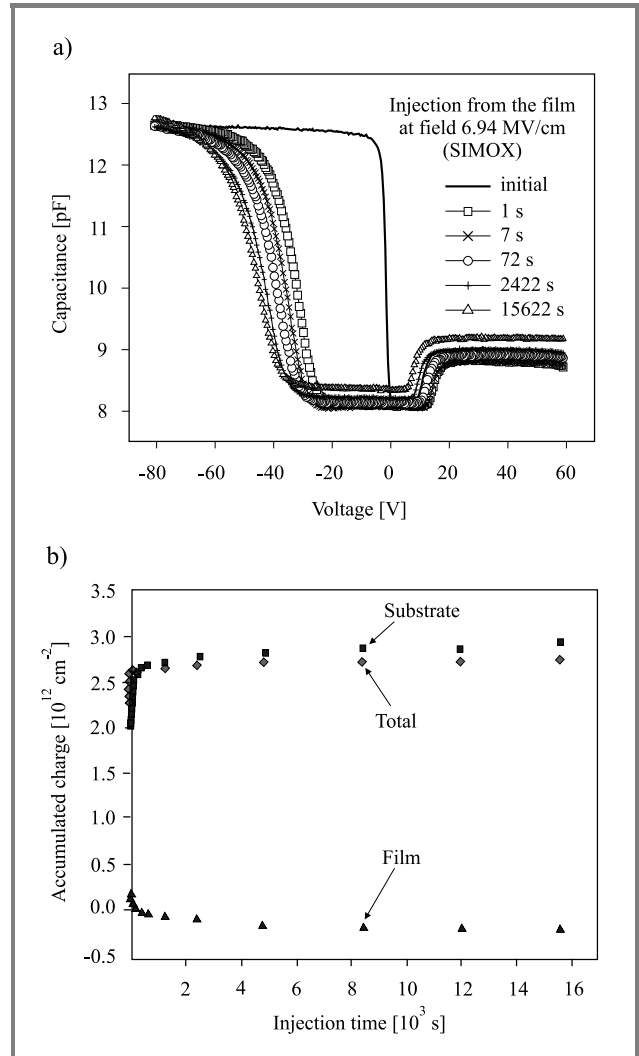


Fig. 5. (a) Capacitance-voltage characteristics of the SIMOX SOI structure with the electron injection time as a parameter; (b) charge accumulated in the BOX as a function of electron injection time.

The C-V characteristics allow the determination of the average doping concentration in Si film both for the experimental UNIBOND and SIMOX SOI structures ($N_d = 2.7 \cdot 10^{16} \text{ cm}^{-3}$ and $N_a = 2.4 \cdot 10^{16} \text{ cm}^{-3}$, respectively). Additionally, it is possible to find the flat-band and mid-gap voltages for the BOX/substrate and the BOX/film interface. The peculiarities of the calculations needed to determine the above mentioned parameters for the n-Si film/BOX/p-Si substrate and the p-Si film/BOX/p-Si substrate SOI structures have been presented elsewhere [20, 21].

Table 3
Parameters of generated positive charge for different oxides (at field $E = 6.25 \cdot 10^6$ V/cm)

Material	Direction of injection	Q_{acc}^{∞} [10^{11}cm^{-2}]	σ^+ [10^{-16}cm^2]	$\eta(0)$ [10^{-4}]	T_{ann} [$^{\circ}\text{C}$]
UNIBOND	Film	2.6	12.0	3.0	400
	Substrate	4.0	4.3	1.7	
SIMOX	Film	24.0	28.0	67.0	> 400
	Substrate	9.6	7.4	7.1	
Gate oxides	Si substrate [22]	78.0	0.25	2.0	150–400
	Si substrate [17]	0.17	5.8	0.09	

It is worth mentioning that the value of the initial positive charge in the BOX (determined from the difference in the flat-band voltages of the BOX/Si film and the BOX/Si substrate interfaces) was about the same for both the experimental UNIBOND and the SIMOX SOI capacitors and was not higher than $1 \cdot 10^{12} \text{cm}^{-2}$. This positive charge was initially located mainly near the BOX/silicon film interface. Figures 4a and 5a demonstrate a rather different behavior of the experimental UNIBOND and the SIMOX structures under high-field electron injection, but, as it is described later, both materials are similar in the main trends of the charge build-up. From the C-V characteristics of SOI capacitors the accumulated charge in the BOX during high-field electron injection was calculated using the technique described in [24]. The charge accumulated in the BOX of experimental UNIBOND and SIMOX SOI structures during the electron injection from the Si film, is shown as a function of the injection time in Figs. 4b and 5b, respectively.

In the case of the experimental UNIBOND structure only a decrease of the positive charge at the BOX/film interface due to the trapping of negative charge is observed during first minutes of injection (Fig. 4). Then, some positive charge begins to build up near the BOX/substrate interface. Thus the dynamic characteristics of the charge accumulation in such structures can be divided into two regions, one of which is related to negative charge trapping near the film and the other to positive charge accumulation near the interface with the substrate (see Fig. 4b). It should be noted that for the experimental UNIBOND structures positive charge accumulation occurs predominantly near the BOX/substrate interface during the electron injection from both the film and the substrate. The concentration of this positive charge in the UNIBOND structures at the electric field of 6.25 MV/cm is near $3 \cdot 10 \text{cm}^{-2}$ for the injection from the film and about $4 \cdot 10^{11} \text{cm}^{-2}$ for the injection from the substrate (Table 3).

In the case of SIMOX structures the C-V plots after stress indicate shifts mainly due to the build-up of positive charge which is localized predominantly near the BOX/substrate interface (see Fig. 5a). After 2 seconds of electron injection from the Si film the value of positive charge at the BOX/substrate interface is about $2.2 \cdot 10^{12} \text{cm}^{-2}$ in contrast to about $2 \cdot 10^{11} \text{cm}^{-2}$ at the BOX/silicon film one. Moreover, from Fig. 5b it is clearly seen, that most of the positive

charge is created very quickly, during the first seconds, in strong contrast to the experimental UNIBOND material. It should also be pointed out that positive charge accumulates in the BOX predominantly near the interface with the substrate during electron injection from both the Si film and the Si substrate, just as in experimental UNIBOND structures. This indicates that this interface is more imperfect than the BOX/silicon film one for both SOI materials. Then, at the later stages of the injection, the positive charge accumulation in the BOX is also accompanied by the trapping of the negative charge near the film interface, or a shift of the positive charge from the film to the substrate interface (see Fig. 5b). This may be seen in the C-V plots as a small negative shift of the part related to the BOX/film interface. The first phenomenon is probably dominant because the I-t characteristics, presented in Fig. 6, show consid-

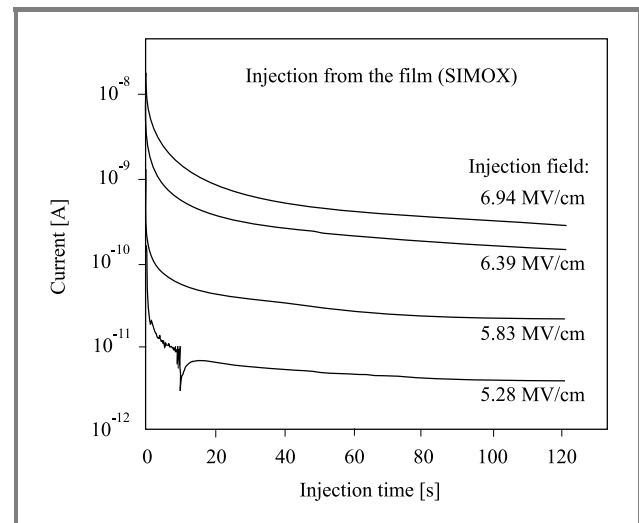


Fig. 6. Current relaxation during the injection of electrons from the film into the SIMOX BOX with the injection field as a parameter.

erable current decrease during the electron injection from the Si film into the BOX. Thus, the positive charge generation and negative charge trapping occur at the same time during the electron injection in the BOX of SIMOX SOI structure, and in this case the concept of centroid charge does not work. However, since these processes occur at

different BOX interfaces they can be studied independently using the BOX/substrate and the BOX/film parts of the C-V characteristics.

In the case of low trapping, electron capture and positive charge accumulation can be expressed in the following way [23]:

$$Q_{acc} = Q_{acc}^{\infty} \{1 - \exp[-\sigma_i Q_{inj}(t)]\}, \quad (3)$$

where Q_{acc}^{∞} is the maximum concentration of accumulated charge determined from the C-V curves shifts, σ_i is the effective cross section of the process, $Q_{inj}(t)$ is the number of injected electrons and can be calculated by the current integration of I-t characteristics registered during electron injection.

From the Q_{acc} vs. Q_{inj} characteristics it is possible to determine independently both the maximum concentration of trapped or generated charge and the process cross section. The value of the maximum concentration is determined from the saturation level of these characteristics. Once the maximum concentration is known, one can calculate the cross section from the slope of the initial part of such a dependence in a following manner:

$$\eta = \left. \frac{dQ_{acc}(t)}{dQ_{inj}(t)} \right|_{Q_{inj} \rightarrow 0} = Q_{acc}^{\infty} \sigma_i, \quad (4)$$

where η is the efficiency of charge accumulation.

Since electron trapping occurs mainly near the BOX/film interface, electron trap parameters estimated from the $Q_{acc}^{film} = f(Q_{inj})$ dependence were approximately the same for both the experimental UNIBOND and the SIMOX structures ($Q_{acc,el}^{\infty} \sim (4-6) \cdot 10^{11} \text{cm}^{-2}$ and $\sigma_e \sim (2-4) \cdot 10^{15} \text{cm}^2$). Electron traps with similar cross sections ($\sim (2-4) \cdot 10^{15} \text{cm}^2$) were found in the gate oxide subjected to different types of radiation [24] and in the BOX of vacuum ultraviolet irradiated UNIBOND and triple implanted SIMOX SOI structures [25]. Traps with similar cross-sections have not been observed in virgin BOX, when silicon film was removed before metal electrode deposition. In our case, we may be possibly dealing with negative charge traps generated during metal gate deposition performed in the laboratory. This process may have resulted in a rather high concentration of electron traps at the top BOX interface. We think, therefore, that these traps are not related to the nature of the buried oxide of the experimental UNIBOND and SIMOX SOI structures.

The parameters of positive charge creation in the BOX of experimental UNIBOND and SIMOX structures for electron injection both from the film and from the substrate obtained using the $Q_{acc} = f(Q_{inj})$ dependence are summarized in Table 3. It can be seen that the efficiency of positive charge creation in the BOX of the SIMOX material is higher than in the UNIBOND structures, which further confirms that the quality of SIMOX buried oxides is worse. Moreover, it should be pointed out that the maximum concentration of the injection-induced positive charge in the SIMOX BOX is higher than in UNIBOND ones by

an order of magnitude, which is consistent with the above conclusion, too.

Thermal annealing of generated positive charge. Removal of the generated positive charge in the BOX of experimental UNIBOND and SIMOX SOI structures by thermal heating was studied by annealing the samples both in isochronal and isothermal modes [26]. After each annealing step, the sample was cooled rapidly in order to record the room-temperature C-V characteristics from which the mid-gap voltage shifts were determined. The anneal-induced removal of the generated positive charge for different samples is depicted in Fig. 7 as a function of the annealing temperature.

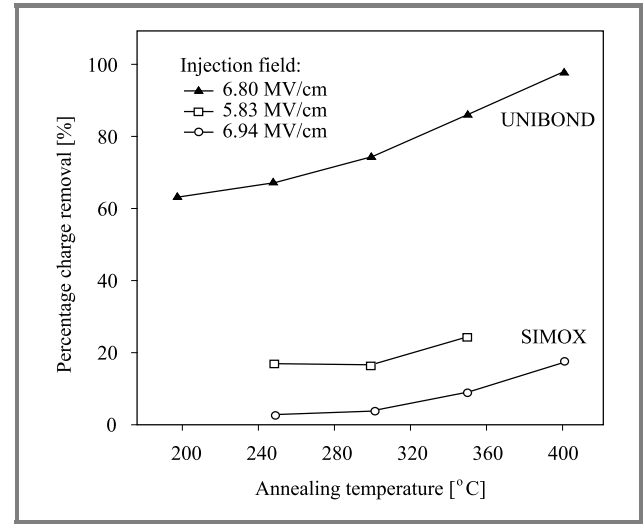


Fig. 7. Annealing of the injection-induced positive charge in the BOX of UNIBOND and SIMOX SOI structures.

From Fig. 7 it is obvious that the positive charge created during the electron injection into the experimental UNIBOND BOX has been almost completely removed after a 15 min. anneal at temperatures up to 400°C. The positive charge generated in a thermal gate oxide is also completely removed when the temperatures of annealing range from 150 to 400°C. In the case of the SIMOX BOX no more than 30% of the total accumulated charge is removed even if the annealing temperature is as high as 400°C. Furthermore, the positive charge generated in the SIMOX BOX at higher electric field is more thermally stable than that generated at lower field.

High thermal stability of positively charged defects created during the electron injection in the SIMOX BOX indicates a more complicated structure of these defects in comparison with that in the thermal gate oxide and in the experimental UNIBOND BOX. Additionally, increased thermal stability of the positive charge generated in the SIMOX BOX at high electric fields suggests the creation of more complicated defects in the BOX than those at lower fields. Thus, it is reasonable to assume that the generation of positive charge during high-field electron injection into the SIMOX BOX occurs simultaneously with the creation of new defects from the precursor sites.

Mechanisms of positive charge generation. First of all, it should be noted that for experimental UNIBOND and SIMOX materials electron injection both from the film and the substrate leads to positive charge generation in the BOX always near the BOX/substrate interface. The obtained results can testify to the absence of trap creation mechanism [27], because in that case the positive charge has to be created always near the anode, independently of the direction of electron injection.

As it can be seen from Table 3, for the **experimental UNIBOND SOI material** the maximum concentration of the generated positive charge is approximately equal and even a little higher for electron injection from the substrate than from the film. In this case it is possible to suggest that **anode hole injection (AHI)** [28] or **band-to-band impact ionization (BTBI)** [29, 30] mechanisms exist in the experimental UNIBOND SOI structure at high electric fields. Detailed overview of positive charge generation mechanisms in the BOX of SOI structures is presented in [14].

Since there was no analytic expression for the hole-generation probability in the case of anode hole injection mechanism in the paper by DiMaria *et al.* [28], we numerically approximated the data presented in Fig. 6 of this paper, and obtained the following result:

$$\alpha_{AHI}(E) = \alpha_{AHI}^0 (E/E_{th}^{AHI} - 1)^{6.2}, \quad (5)$$

where $\alpha_{AHI}^0 = 1.58 \cdot 10^{-8}$ and $E_{th}^{AHI} = 1.1$ MV/cm, which coincides with the threshold of the exponential field dependence in Fishetti's paper [17].

Holes injected from the anode are swept across the whole oxide film for both directions of FN electron injection. Therefore, regardless of the polarity of electron injection into the oxide and hole trap localization in the oxide, no asymmetry is expected for the AHI mechanism. Thus, in this case $P_{neg}/P_{pos} \approx 1$. Some asymmetry may arise from the variation in the efficiency of hole injection for various contacts.

The existence of AHI in thick oxides has been reported in some papers [17, 28]. AHI modeling, performed by DiMaria *et al.* [28], predicts a sufficiently strong dependence of the probability of hole generation (see Eq. (5)). Therefore, the observed increase of the maximum concentration of the generated positive charge, $Q_{acc,holes}^\infty$, with the growth of the electric field may be associated with an increase of the hole-generation probability and a decrease of the recombination cross-section for electrons, $\sigma_r \sim E^{-3}$.

In the case of the BTBI mechanism, the hole-generation probability has been shown to be strongly dependent on the electric field [29]. Moreover, this dependence is considerably different from that for anode hole injection:

$$\alpha_{BTBI}(E) = \alpha_{BTBI}^0 (E/E_{th}^{BTBI} - 1)^4, \quad (6)$$

where $\alpha_{BTBI}^0(E) = 3.6$ (for thick oxide, $d = 400$ nm), and E_{th}^{BTBI} is the threshold electric field for the BTBI ($E_{th}^{BTBI} = 6.4$ MV/cm).

Since BTBI holes are created in the bulk of thick oxides, in the case of asymmetric hole-trap distribution the asymmetry in hole trapping will also be observed during electron injection with different FN electric field polarity. In the case of the UNIBOND structures, for example, where a non-uniform distribution of hole traps with a maximum near the BOX/silicon substrate interface is observed, $P_{neg}/P_{pos} \ll 1$ for the BTBI mechanism. Usually, in thick oxides the processes of the BTBI occur simultaneously with the AHI [22].

Experimental results and theoretical curves describing AHI and BTBI as functions of the average electric field in the BOX are shown in Fig. 8. The theoretical curves for AHI and BTBI are extracted from the papers of DiMaria *et al.* [28] and Arnold *et al.* [29], respectively. The efficiency of positive charge generation, η , was obtained directly from the experimental $Q_{acc} = f(Q)_{inj}$ characteristics. The generation cross section, σ^+ , was calculated from Eq. (4) and the known values of the maximum generated charge presented in Fig. 8a.

The theoretical generation-efficiency curves were calculated from the following expression [14]:

$$\eta(E) = \alpha(E) \sigma_p Q_p = \alpha_0 (E/E_{th} - 1)^n \sigma_p Q_p. \quad (7)$$

The curves describing the maximum generated charge, as well as the characteristics of the generation cross-section, were obtained using equations (28a) and (28b) of [14]. The hole-capture cross-section was $\sigma_p = 1 \cdot 10^{-14}$ cm⁻². Other parameters, such as α_0 , E_{th} , and n for both AHI and BTBI mechanisms were presented above, $Q_p = 5 \cdot 10^{12}$ cm⁻².

A comparison of the experimental data with the theoretical curves for AHI and BTBI for all three parameters of positive-charge generation in the case of electron injection from the film shows that the experimental values are significantly higher than the theoretical ones (see Fig. 8). This indicates that the quality of the experimental UNIBOND material investigated in this paper is not at the level of thermal oxides. Simultaneously, one may notice that the qualitative behavior of the experimental data is similar to the theoretical calculations.

Fitting the theoretical AHI characteristics to the experimental data presented in Fig. 8b allows the extraction of the generation efficiency in the form $\eta(E) = \eta_0 (E/E_{th}^{exp} - 1)^{14.3}$, where $\eta_0 = 1.9 \cdot 10^{-20}$ and $E_{th}^{exp} = 0.4$ MV/cm. From the experimental data for generation cross-section at low fields, presented in Fig. 8c, the recombination cross-section has been obtained as $\sigma_r(E) = \sigma_r^0 E^{-1.5}$, where $\sigma_r^0 = 1.4 \cdot 10^{-14}$ MV^{1.5} cm^{0.5}. As it can be seen from Eq. (7), the dependence of the generation efficiency on the electric field is determined by the dependence of hole-generation probability, α , on the electric field. Thus, we can write, that $\alpha_{AHI}(E) = \alpha_{AHI}^0 (E/E_{th}^{exp} - 1)^{14.3}$, where the exponential is considerably higher than that extracted from DiMaria's data [28] and present in Eq. (5).

However by employment of both AHI and BTBI mechanisms it is possible to obtain a good agreement between the experimental results and theory (see Fig. 8). In this case the best agreement was obtained using Eqs. (5) and (6)

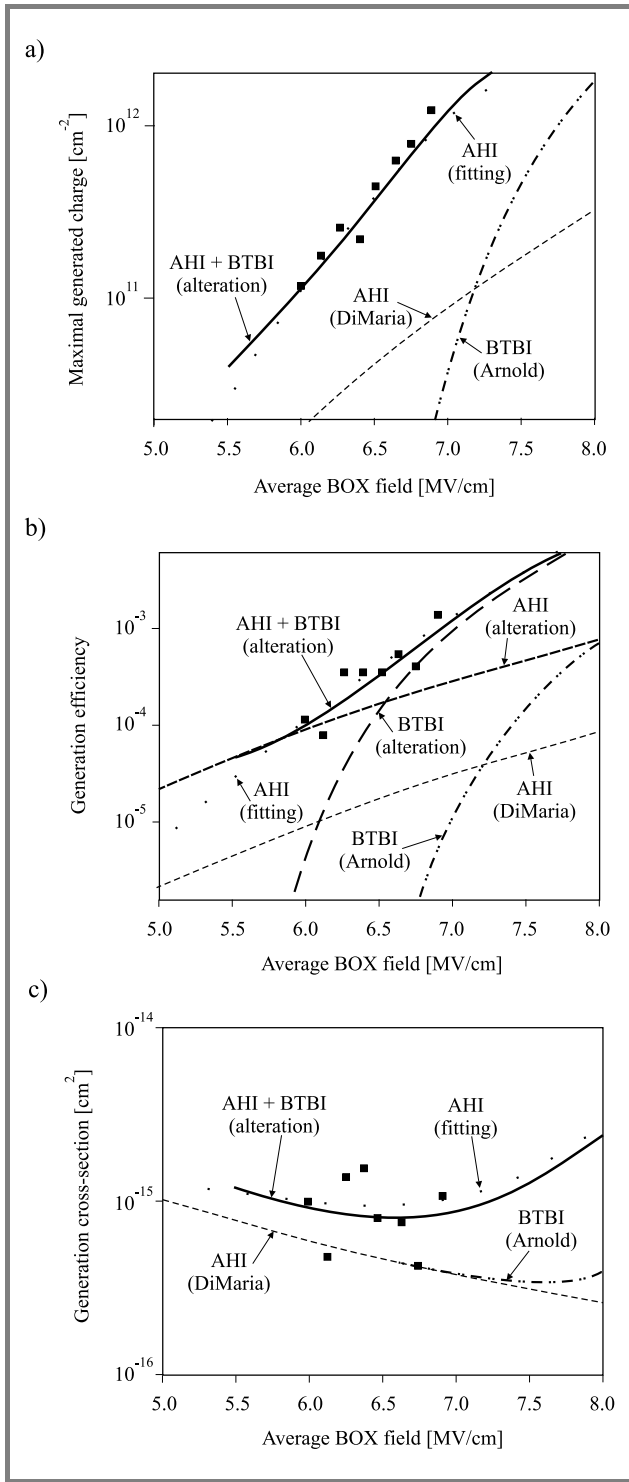


Fig. 8. Parameters of positive charge generation in the BOX of the experimental UNIBOND structures as a function of average BOX electric field: (a) maximum generated charge; (b) generation efficiency; (c) generation cross-section. Theoretical curves for AHI and BTBI mechanisms are plotted after DiMaria *et al.* [28] and Arnold *et al.* [29], respectively.

to calculate the hole-generation probability, with the following parameters: $\alpha_{AHI}^0 = 1.4 \cdot 10^{-8}$, $E_{th}^{AHI} = 0.8$ MV/cm, $\alpha_{BTBI}^0 = 3.6$, $E_{th}^{BTBI} = 5.6$ MV/cm. One can see that in the case of the experimental UNIBOND SOI structure

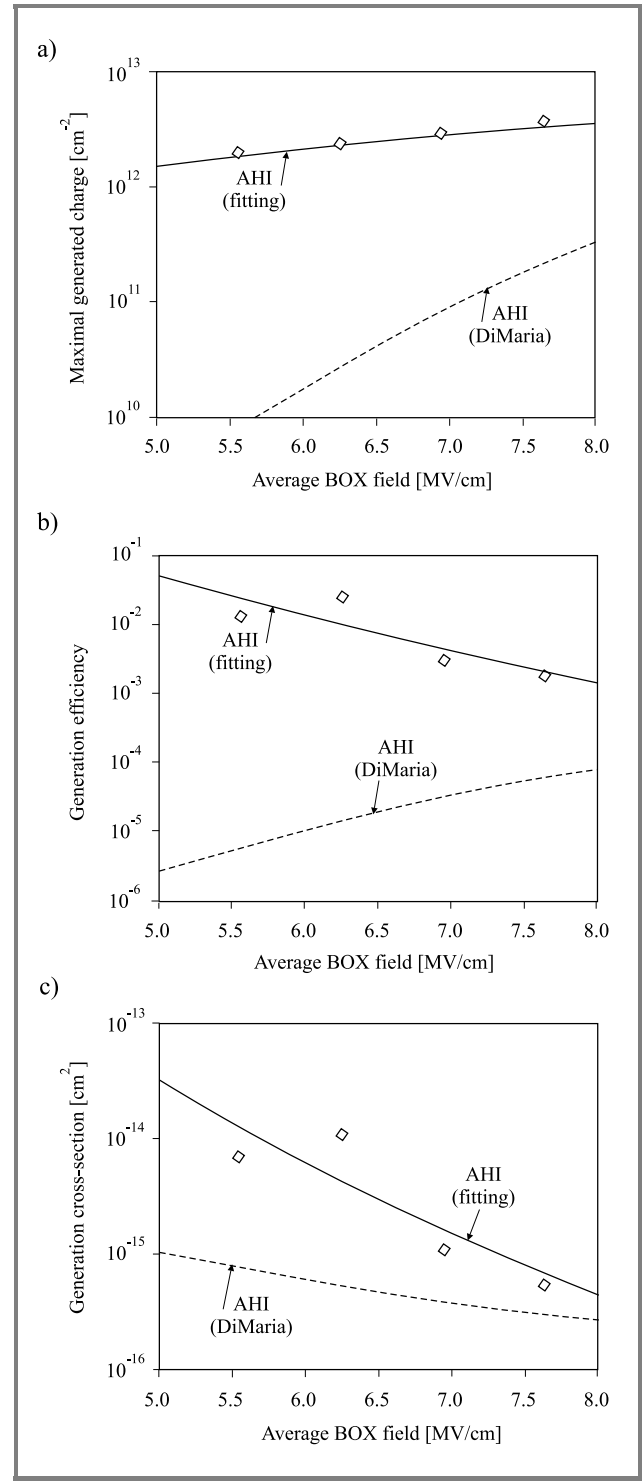


Fig. 9. Parameters of positive charge generation in the BOX of SIMOX structures as a function of the average BOX electric field: (a) maximum generated charge; (b) generation efficiency; (c) generation cross section. Theoretical curves for AHI mechanism are plotted after DiMaria *et al.* [28].

the threshold electric fields for the beginning of AHI and BTBI processes are slightly lower than those reported in [17, 30]. This can be explained by a considerable thickness of the BOX (nearly 400 nm) and

disturbed BOX/substrate interface. Other parameters in the model are similar to those proposed in the paper of DiMaria *et al.* [28]: $\sigma_p = 1.5 \cdot 10^{-14} \text{ cm}^2$, $\sigma_r^0 = 2 \cdot 10^{-13} \text{ MV}^3 \text{ cm}^{-1}$, and $Q_p = 4 \cdot 10^{12} \text{ cm}^{-2}$.

In the case of the **SIMOX material** the maximum charge generated during the electron injection from the film is much higher than that generated during the electron injection from the substrate (see Table 2). Since for this material the structural quality of the BOX/substrate interface is considerably worse than that of the BOX/film interface, the AHI mechanism can explain the observed behavior. As it is shown in Fig. 9, the fitting of the theoretical AHI curves to the experimental data allows good agreement to be obtained. In this case, however, the hole-capture cross-section σ_p and the electron recombination cross-section σ_r have to be strongly dependent on the electric field ($\sigma_p \sim E^{-14.9}$ and $\sigma_r \sim E^{-9.3}$), which is physically impossible. It should be noted, though, that in the SIMOX material an increase of the electric field results in an increase of the thermal stability of the trapped positive charge (see above). This indicates that a new defect complex is created. Thus, we may conclude that the apparent strong dependence of σ_p and σ_r on the electric field is possibly associated with the transformation of the initial traps or generation of new hole and electron traps for with smaller capture cross-section than that of the initial traps. Trap transformation in the SIMOX BOX during the high field electron injection is a process that is physically probable. Indeed, the amorphous oxide network in the SIMOX BOX is very strained [5, 7] and contains a lot of precursor sites for charge trapping. In the trapping process, carriers can break the weak and strained bonds, creating trapped charge [31, 32].

4. Conclusions

Processes of charge transfer and positive charge generation during high-field electron injection in the buried oxides of experimental UNIBOND and SIMOX SOI structures have been investigated.

It was shown that high-field electron injection into the BOX of both kinds of SOI structures may be described using trap-assisted tunneling mechanism on condition that the peculiarities of each kind of SOI structures are taken into account. In the case of the injection from the Si film into the BOX of the experimental UNIBOND structure it is necessary to consider simultaneously direct tunneling because the quality of this interface is very high. For the SIMOX structure it is necessary to take into account the influence of the positive charge generated in the BOX on the processes of injection. Estimation of the trap concentrations in the vicinity of each interface of both experimental UNIBOND and SIMOX SOI structures obtained from the TAT fitting confirms that the quality of the substrate/BOX interface in comparison with that of the film/BOX interface is worse for both types of structures.

It was demonstrated that in both types of SOI structures positive charge in the BOX is generated mainly near the

BOX/substrate interface, which confirms that the quality of this interface is worse. In the BOX of the SOI structures fabricated using the experimental UNIBOND technique the positive charge is generated by anode hole injection and band-to-band impact ionization mechanisms with lower threshold voltages than in the case of thin gate oxides. In the case of the SIMOX material the predominant generation mechanism is determined to be the anode hole injection with simultaneous dynamic transformation of the precursor sites into traps in the strained structure of the BOX under the influence of hot electrons. Positive charge is generated more effectively in the SIMOX SOI structures than in the experimental UNIBOND ones, and this charge is shown to be much more thermally stable in the BOX of SIMOX structures. These facts confirm that the quality of the SIMOX BOX is worse when compared to that of the experimental UNIBOND BOX.

Acknowledgments

This work was supported by STCU project no. 2332. The authors thank Dr. M. Bruel and Dr. B. Aspar (CEA/LETI, Grenoble, France) for providing the experimental UNIBOND SOI wafers. The authors also acknowledge Dr. H. Moriceau and Dr. B. Aspar for helpful discussions.

References

- [1] T. Ouisse, S. Cristoloveanu, and G. Borel, "Hot-carrier-induced degradation of the back interface in short-channel silicon-on-insulator MOSFETs", *IEEE Electron. Dev. Lett.*, vol. 12, pp. 290–292, 1991.
- [2] M. Bruel, "Smart-Cut[®] technology: basic mechanisms and applications", in *Perspectives, Science and Technology for Novel Silicon-on-Insulator Devices*, P. L. F. Hemment, V. S. Lysenko, and A. N. Nazarov, Eds. Dordrecht: Kluwer, 2000, pp. 1–15.
- [3] S. Kranse, M. Anc, and P. Roitman, "Evaluation and future trends of SIMOX material", *MRS Bull.*, vol. 23, p. 25–29, 1998.
- [4] V. V. Afanas'ev, A. Stesmans, and H. E. Twigg, "Epitaxial growth of SiO₂ produced in silicon by oxygen ion implantation", *Phys. Rev. Lett.*, vol. 77, pp. 4206–4209, 1996.
- [5] V. V. Afanas'ev, A. Stesmans, A. G. Revesz, and H. L. Hughes, "Structural inhomogeneity and silicon enrichment of buried SiO₂ layers formed by oxygen implantation in silicon", *J. Appl. Phys.*, vol. 82, pp. 2184–2199, 1997.
- [6] K. Vanhensden and A. Stesmans, "Similarities between separation by implanted oxygen and bonded and etch-back silicon-on-insulator material as revealed by electron spin resonance", in *Silicon-on-Insulator Technology and Devices V*, S. Cristoloveanu *et al.*, Eds. Electrochemical Society, 1994, pp. 197–202.
- [7] A. G. Revesz and H. L. Hughes, "Properties of the buried oxide layer in SIMOX structures", *Microelectron. Eng.*, vol. 36, pp. 343–350, 1997.
- [8] V. V. Afanas'ev, A. Stesmans, A. G. Revesz, and H. L. Hughes, "Mechanism for Si island retention in buried SiO₂ layers formed by oxygen ion implantation", *Appl. Phys. Lett.*, vol. 71, no. 15, pp. 2106–2108, 1997.
- [9] M. Lenzlinger and E. H. Snow, "Fowler-Nordheim tunneling into thermally grown SiO₂", *J. Appl. Phys.*, vol. 40, pp. 278–283, 1969.
- [10] Z. A. Weinberg, "Tunneling of electrons from Si into thermally grown SiO₂", *Solid State Electron.*, vol. 20, pp. 11–18, 1976.

[11] Z. A. Weinberg and A. Harstein, "Effect of silicon orientation and hydrogen annealing on tunneling from Si into SiO₂", *J. Appl. Phys.*, vol. 54, pp. 2517–2521, 1983.

[12] C. M. Osburn and E. J. Weitzman, "Electrical conduction and dielectric breakdown in silicon dioxide films on silicon", *J. Electrochem. Soc.*, vol. 119, pp. 603–609, 1972.

[13] S. Hall and S. P. Wainwright, "On electron conduction and trapping in SIMOX dielectric", *J. Electrochem. Soc.*, vol. 143, pp. 3354–3358, 1996.

[14] A. N. Nazarov, V. I. Kilchytska, and I. P. Barchuk, "Charge carrier injection and trapping in the buried oxides of SOI structures", in *Progress in SOI Structures and Devices Operating at Extreme Conditions*, F. Balestra, A. Nazarov, and V. S. Lysenko, Eds. Dordrecht: Kluwer, 2002, pp. 139–158.

[15] C. Svensson and I. Lundström, "Trap-assisted charge injection in MNOS structure", *J. Appl. Phys.*, vol. 44, pp. 4657–4663, 1973.

[16] F. Stern, "Self-consistent results for *n*-type Si inversion layers", *Phys. Rev. B*, vol. 5, pp. 4891–4899, 1972.

[17] M. V. Fischetti, "Generation of positive charge in silicon dioxide during avalanche and tunnel electron injection", *J. Appl. Phys.*, vol. 57, pp. 2860–2878, 1985.

[18] C. Chen, W. L. Wilson, and M. Smayling, "Tunneling induced charge generation in SiO₂ thin film", *J. Appl. Phys.*, vol. 83, pp. 3898–3905, 1998.

[19] S. Bengtsson, A. Jauhiainen, and O. Engstrom, "Oxide degradation of wafer bonded metal-oxide-semiconductor capacitors following Fowler-Nordheim electron injection", *J. Electrochem. Soc.*, vol. 139, pp. 2302–2306, 1992.

[20] A. N. Nazarov, V. S. Lysenko, V. A. Gusev, and V. I. Kilchitskaya, "C-V and thermally activated investigations of ZMR SOI meza structures", in *Silicon-on-Insulator Technology and Devices V*, S. Cristoloveanu *et al.*, Eds. Electrochemical Society, 1994, pp. 236–244.

[21] T. E. Rudenko, A. N. Rudenko, A. N. Nazarov, V. S. Lysenko, and V. I. Kilchitskaya, "Ehlektrifizicheskie svojjstva KNI-struktur: metody issledovanija i ehksperimentalnye rezultaty", *Mikroelektronika*, vol. 23, no. 6, pp. 18–31, 1994.

[22] M. V. Fischetti, "Model for the generation of positive charge at the Si-SiO₂ interface based on hot-hole injection from anode", *Phys. Rev. B*, vol. 31, pp. 2099–2113, 1985.

[23] V. V. Afanas'ev and V. K. Adamchuk, "Injection spectroscopy of localized states in thin insulating layers on semiconductor surfaces", *Prog. Surf. Sci.*, vol. 47, pp. 301–394, 1994.

[24] J. M. Aitken and D. R. Young, "Electron trapping by radiation-induced charge in MOS devices", *J. Appl. Phys.*, vol. 47, p. 1196, 1976.

[25] V. V. Afanas'ev, A. Stesmans, A. G. Revesz, and H. L. Hughes, "Trap generation in buried oxides of silicon-on-insulator structures by vacuum ultraviolet radiation", *J. Electrochem. Soc.*, vol. 144, pp. 749–753, 1997.

[26] A. N. Nazarov, V. I. Kilchytska, I. P. Barchuk, A. S. Tkachenko, and S. Ashok, "Radio frequency plasma annealing of positive charge generated by Fowler-Nordheim electron injection in buried oxides in silicon", *J. Vac. Sci. Technol.*, vol. 18, pp. 1254–1261, 2000.

[27] D. A. Buchanan, A. D. Marwick, D. J. DiMaria, and L. Dori, "Hot-electron-induced hydrogen redistribution and defect generation in metal-oxide-semiconductor capacitors", *J. Appl. Phys.*, vol. 76, pp. 3595–3608, 1994.

[28] D. J. DiMaria, E. Cartier, and D. A. Buchanan, "Anode hole injection and trapping in silicon dioxide", *J. Appl. Phys.*, vol. 80, pp. 304–317, 1996.

[29] D. Arnold, E. Cartier, and D. J. DiMaria, "Theory of high-field electron transport and impact ionization in silicon dioxide", *Phys. Rev. B*, vol. 49, pp. 10278–10297, 1994.

[30] D. J. DiMaria, "Defect production, degradation, and breakdown of silicon dioxide films", *Solid State Electron.*, vol. 41, pp. 957–965, 1999.

[31] S. K. Lai, "Interface trap generation in silicon dioxide when electrons are captured by trapped holes", *J. Appl. Phys.*, vol. 54, p. 2540, 1983.

[32] G. W. McPherson, R. B. Khamankar, and A. Shanware, "Complementary model for intrinsic time-dependent dielectric breakdown in SiO₂ dielectrics", *J. Appl. Phys.*, vol. 88, pp. 5351–5359, 2000.



Alexei N. Nazarov graduated *summa cum laude* from Kiev Polytechnical Institute (Kiev, Ukraine) in 1968, in the field of electronics engineering. He received the Ph.D. and D.Sc. degrees in physics and mathematics from the Institute of Semiconductor Physics (ISP), NASU, Kiev, Ukraine, in 1982 and 1993, respectively. His

D.Sc. research was on physics of hydrogen plasma interaction with semiconductor materials and devices. He is now with the Department of Optoelectronics, ISP NASU as leading reseacher and a Professor at National Technical University (KPI) giving courses on "Microelectronics and Nanotechnology". Dr. Nazarov is a Senior Member of IEEE Society and a Member of Electrochemical Society. He is currently involved in the development of silicon-on-insulator CMOS devices operating in harsh conditions and R&D of Si-based optoelectronic devices.

e-mail: nazarov@lab15.kiev.ua
 Institute of Semiconductor Physics
 National Academy of Sciences of Ukraine
 03028, Prospect Nauky, 45, Kiev, Ukraine



Yuri Houk received the M.Sc. degree in applied physics from National Technical University of Ukraine in 2002. His Master's project was carried out in the Institute of Semiconductor Physics, National Academy of Sciences of Ukraine (ISP, NASU), and was devoted to charge transport and trapping in buried oxide of

SOI structures. Since 2002 he has been participating in the Ph.D. programme of ISP, NASU. The subject of his Ph.D. investigations is charge transport and trapping in the buried oxides of SOI structures and MOSFETs. In 2001 he joined ISP as a researcher assistant. He is involved in the investigation of charge injection and trapping processes in buried oxide of SOI structures and in the investigation of radiation hardness of MOSFETs fabricated on the SOI basis.

e-mail: houk@lab15.kiev.ua
 Institute of Semiconductor Physics
 National Academy of Sciences of Ukraine
 03028, Prospect Nauky, 45, Kiev, Ukraine



Valeriya I. Kilchytska received the M.Sc. degree in solid-state electronics and Ph.D. degree in semiconductors and dielectrics physics, from Kiev University in 1992 and in 1997, respectively. She performed her Ph.D. research in Institute of Semiconductor Physics, Kiev, Ukraine. Her Ph.D. work was devoted to the investigation of

electrical and radiation properties of SOI structures, particularly to the improving of the radiation hardness of buried dielectric. From 1997 to 2001 she continued to work in the

Institute of Semiconductor Physics, first as researcher assistant and then as researcher. She has been involved in the high-temperature characterization of SOI devices and in the investigation of bias-temperature and injection processes in the buried oxides in SOI structures. She is currently working in the Microelectronics Laboratory of the Université Catholique de Louvain, Louvain-la-Neuve, Belgium. Her current research interest is focused on the room- and high-temperature characterization and simulation of advanced deep sub-micrometer SOI devices.

e-mail: lerka@dice.ucl.ac.be

Institute of Semiconductor Physics
National Academy of Sciences of Ukraine
03028, Prospect Nauky, 45, Kiev, Ukraine